Macromolecular Materials and Engineering
Open Access
www.mame-journal.de

Lignin/Poly(vinylpyrrolidone) Multifilament Fibers Dry-Spun from Water as Carbon Fiber Precursors

Philipp Kreis, Erik Frank, Bernd Claußß, Volker Bauch, Heiko Stolpmann, Lisa Kuske, Tanja Schneck, Simon König, and Michael R. Buchmeiser**

The preparation of lignin-based carbon fibers by dry spinning from aqueous solution followed by stabilization and continuous carbonization to endless yarns is reported. The influence of carbonization temperature and draw ratio on the morphology and mechanical properties of the final carbon fibers is investigated by single-fiber testing, wide-angle X-ray scattering, scanning electron microscopy, and Raman spectroscopy. A draw ratio of 5% (1.05) with a carbonization temperature of 1400 °C leads to the best mechanical properties. The resulting multifilament carbon fibers have an average diameter between 10–12 µm, an average tensile strength of 1.30 ± 0.32 GPa, a Young's modulus of 101 ± 18 GPa, and an elongation at break of 1.31 ± 0.23%. The maximum Weibull strength (σ_0) is 1.04 GPa with a Weibull modulus (*m*) of 5.1. The use of a water-soluble system is economically advantageous; also, unlike melt-spun lignin fibers, the dry-spun precursor fibers can be thermally converted without any additional crosslinking step.

1. Introduction

Over the years, carbon fibers (CFs) experienced a continuously increasing demand in mass markets such as automotive, wind energy, and aerospace industries.[1] CFs and their composites combine excellent mechanical properties with low weight, offering a high energy-saving potential.[2] In recent years, significant efforts have been undertaken to reduce CF production costs without compromising on the quality of the fibers. Currently, over 95% of commercially available CFs are produced by carbonizing fossil-fuel based poly(acrylonitrile) (PAN) precursor fibers, the remainder is based on pitch-precursor fibers.[3] PAN-precursor fibers are manufactured by a wet-spinning process using solvents like dimethylsulfoxide, *N*,*N*-dimethylacetamide, or *N*,*N*-dimethylformamide.[4] Due to the high production costs of CFs, the poor carbon footprint and the use of toxic solvents, alternative precursors are being researched intensively.[5] A promising, low cost alternative candidate as CF precursor is lignin, an abundant biopolymer. Lignin is produced as a waste product in paper production and by biorefineries.[6–8] In addition, lignin has high thermal stability and a high carbon yield of 30–40 wt% after carbonization. 50 million tons per year of lignin are produced in paper manufacturing, of which only about 2% are used for commercial applications. The major part of lignin is used as a source of energy in combustion.[9–12] Based on the different pulping processes, lignin is classified into organosolve,[13] Kraft,[14,15] soda lignin, and lignosulfonate.[16] In the sulfite process, the hydroxyl groups of lignin are transformed into sulfonate groups, which makes lignin water-soluble and allow its separation from cellulose in solution. The sulfite process can produce lignin sulfonates with weight-average molecular weights up to several 10.000 g mol^{-1}, since the ether bonds of the ß—O—4 units of lignin are rather stable under acidic conditions.[17] A large number of patents and publications exist for the production of lignin-based CFs.[18–23] Already in the early 1960s, the first processes for the production of carbonized lignin fibers were reported by Otani et al.[24] The lignin fibers were prepared using melt-spinning, dry-spinning, and wet-spinning processes. The most common process is melt-spinning, which uses either special types of lignin or chemically modified lignin, thereby allowing their melt processing.[19,21] The melt-spinning process entails several advantages, such as the absence of solvents and a high take-up speed. Nevertheless, the stabilization of melt spun lignin precursor fibers is difficult, because the fibers are prone to melt or fuse during this process.[16] Alternatively, lignin-based precursor fibers can be prepared by wet-spinning; however, the low molecular weight and amorphous structure of lignin render the process difficult.[17,25–28] In view of these impediments, the dry-spinning of lignin from solution under concomitant evaporation of the solvent has moved into the center of interest. Mansmann et al. reported on the co-spinning of lignosulfonate with polyethylene oxide or acrylic acid-acrylamide copolymers as additives. These

P. Kreis, E. Frank, B. Claußß, V. Bauch, H. Stolpmann, L. Kuske, T. Schneck, S. König, M. R. Buchmeiser
German Institutes of Textile and Fiber Research
Körschtalstraße 26, D-73770 Denkendorf, Germany
E-mail: erik.frank@ditf.de; michael.buchmeiser@ipoc.uni-stuttgart.de
M. R. Buchmeiser
Institute of Polymer Chemistry
University of Stuttgart
Pfaffenwaldring 55, D-70569 Stuttgart, Germany

The ORCID identification number(s) for the author(s) of this article can be found under https://doi.org/10.1002/mame.202300296

DOI: 10.1002/mame.202300296

polymers had to be added to provide spinning dopes that show shear thinning, thereby allowing for the preparation of small-diameter multifilament endless precursor fibers. After stabilization and carbonization, the final CFs had a tensile strength of 0.8 GPa.[29,30] Zhang et al. investigated the dry-spinning of acetylated softwood Kraft lignin with acetone and the influence of the processing temperature and spinning concentration on the processability of the fiber.[22,23] Scanning electron microscopy (SEM) measurements showed that the fiber surface did not have a uniformly round cross-section because of the rapid evaporation of acetone. The fibers exhibited a tensile strength of 1.04 ± 0.10 GPa and a Young's modulus of 52 ± 2 GPa. Since fiber fusion could only be avoided by applying a low heating rate of 0.01 °C min^{-1}, this process proved unsuitable for any large-scale production. Jin et al. reported on the use of fractionated lignin from softwood Kraft lignin and its dry-spinning into fibers using 85% aqueous acetic acid as solvent.[31] The fibers exhibited a strength of 1.39 ± 0.23 GPa and a Young's modulus of 98 ± 5 GPa.

In this study, a novel process is reported in which lignosulfonate multifilament fibers are dry-spun from water on a kg-scale with poly(vinylpyrrolidone) (PVP) as supporting polymer to obtain lignin-based CF multifilament at reasonable processing speeds. Stabilization was performed discontinuously in a drying oven at up to 250 °C applying a heating rate of 1 °C min^{-1}. Carbonization at 1000 to 1600 °C was accomplished in a continuous carbonization process at a processing speed of 0.4 m min^{-1}. The influence of carbonization temperature under draw ratio (DR) on the mechanical properties of the resulting CFs was investigated by single fiber tests, wide-angle X-ray scattering, Raman spectroscopy, and scanning electron microscopy. Compared to other additive polymers, such as polyvinyl alcohol, the precursor fiber can be processed at a higher heating rate in the stabilization process due to the usage of PVP. The reason for this is the thermal behavior of PVP, in particular its glass transition temperature of 171 °C, which allows stabilization of the precursor fibers with heating rates of up to 20 °C min^{-1}. Consequently, the necessary energy for stabilization can be reduced by at least 50% compared to the state of the art. Replacement of organic solvents by water in the spinning process of the precursor reduces the costs for precursor preparation. In view of environmental concerns and increasingly scarce petroleum resources, this study presents a new promising approach to the production of low-cost, environmentally friendly carbon fibers that can find application in industry.

2. Results and Discussion

2.1. Preparation of Precursor Fibers

In preliminary trials, different lignin concentrations between 50 and 80 wt% were investigated for their processability. Even a very high concentration of 80 wt% lignin allowed for a good processability in preliminary spinning trials. However, in terms of fiber quality, diameter, spinning stability, and brittleness, spinning solutions consisting of 60 wt% ammonium lignosulfonates with 40 wt% PVP K30 showed the best properties for precursor handling and carbon fiber properties. The spinning dope was subjected to rheology measurements at four different temperatures between 45 and 15 °C. The resulting master curve for a spinning temperature of 22 °C gave a zero-shear viscosity (η_0) of 475 Pa s (**Figure 1**). The viscoelastic behavior is described by the storage modulus (G') and loss modulus (G''). The loss factor $\tan(\delta) = G''/G'$ was >1 in the measured frequency range, indicating a viscous behavior of the spinning dope. The spinning solution, consisting of 60 wt% ammonium lignosulfonates with 40 wt% PVP K30 in water, was successfully dry-spun at a pilot scale. The dry-spinning process was stable without any yarn breakage or drop formation.

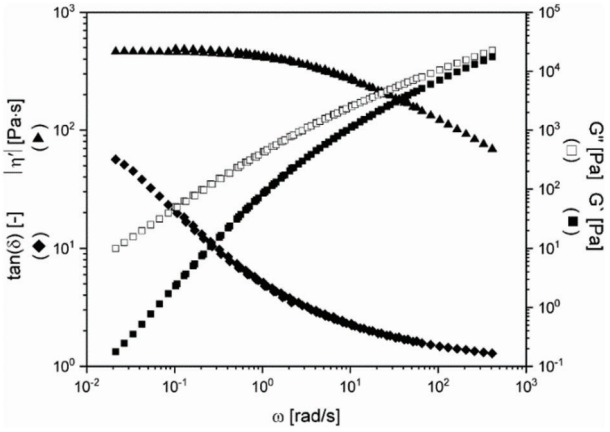

Figure 1. Rheological characterization of a spinning dope with a η_0 of 475 Pa s at 22 °C.

2.2. Stabilization of the Precursor Fibers

Stabilization was carried out discontinuously in a drying oven by heating in air. A temperature at 250 °C was selected as the final temperature for stabilization. Since this precursor does not melt upon heating, a heating rate of 1 °C min^{-1} was successfully applied without causing the fibers to stick together. This represents a significant advantage over melt-spinnable lignin fibers, which first have to be converted from the thermoplastic to the thermoset state. Oxidative crosslinking of lignin in the presence of air resulted in the mechanical properties of the precursor fibers listed in **Table 1**. The tensile strength of the stabilized precursor fibers was 97 ± 6 MPa; the Young's modulus was 5 ± 1 GPa.

2.3. Carbonization

Table 2 shows the influence of the maximum carbonization temperature, chosen between 1000 and 1600 °C, on the

Table 1. Properties of the precursor fibers stabilized at 250 °C applying a heating rate of 1 °C min^{-1}. σ = tensile strength ϵ = elongation at break.

Density [g mL^{-1}]	1.39 ± 0.01
σ [cN tex^{-1}]	7 ± 0.4
σ [MPa]	97 ± 6
Young´s Modulus [cN tex^{-1}]	335 ± 23
Young´s Modulus [GPa]	5 ± 1
ϵ [%]	4.2 ± 0.5
Fineness [dtex]	4.3 ± 0.5
Fineness [µm]	19.9 ± 1.1

Table 2. Properties of CFs carbonized at different maximum temperatures without fiber drawing (DR = 1.00).

Sample ID	Carbonization temperature [°C]	DR	Fineness [µm]	σ_0 [GPa]	Young's Modulus [GPa]	ϵ [%]
CF1000	1000	1.00	13.9 ± 1.6	0.66 ± 0.24	55 ± 12	1.22 ± 0.31
CF1200	1200	1.00	12.7 ± 1.2	0.96 ± 0.23	68 ± 12	1.45 ± 0.24
CF1400	1400	1.00	12.4 ± 2.6	1.00 ± 0.26	74 ± 21	1.42 ± 0.35
CF1600	1600	1.00	13.1 ± 1.0	0.84 ± 0.20	47 ± 10	1.81 ± 0.36

Table 3. Mechanical properties of CFs carbonized at 1400 °C with different DRs. σ_0 = tensile strength; ϵ = elongation at break.

Sample ID	Carbonization temperature [°C]	DR	Fineness [µm]	σ_0 [GPa]	Young's Modulus [GPa]	ϵ [%]
CF1400	1400	1.00	12.4 ± 2.6	1.00 ± 0.26	74 ± 21	1.42 ± 0.35
CF1400.2	1400	1.01	10.9 ± 0.9	1.18 ± 0.32	91 ± 16	1.33 ± 0.28
CF1400.3	1400	1.05	11.1 ± 0.6	1.30 ± 0.32	101 ± 18	1.31 ± 0.23
T300 (PAN-derived)[34]	—	—	7.0	3.0	200	1.5

mechanical properties of the CFs (Figure S5, Supporting Information).

The mechanical properties of the lignin-based CFs were determined by single filament tensile testing. The stress–strain curves of CFs with different draw ratios are given in Figure S6, Supporting Information. The CFs carbonized at 1400 °C showed the highest tensile strength, similar to what is observed in the carbonization of PAN fibers.[32] Thus, increasing the carbonization temperature from 1000 to 1200 °C and 1400 °C, respectively, resulted in an increase in tensile strength of the CFs from 0.66 to 1.0 GPa (+30%) and an increase in Young's modulus from 55 to 74 GPa (+26%). CF1600 fibers carbonized at 1600 °C experienced a decrease in strength from 1.0 to 0.8 GPa (−20%) and in the Young's modulus of from 74 to 47 GPa (−37%). To improve the mechanical properties, carbonization was carried out at a temperature of 1400 °C applying draw ratios (DRs) of 1.01 and 1.05, respectively.[3,33] The mechanical properties significantly increased with increasing DR (**Table 3**) reaching a tensile strength of 1.3 ± 0.32 GPa (+23%) with a Young's modulus of 101 ± 18 GPa (+26%) applying a DR of 1.05. Concomitantly, a decrease in elongation at break from 1.42% to 1.31% was observed. At higher draw ratios >5% some fiber breaks occurred because the yarn quality along the fiber bundles was not fully constant. Nonetheless, the data presented here clearly show that higher draw ratios can significantly improve the mechanical properties of the CFs. A reduction in the mechanical properties of CFs can be caused by defects resulting from ash impurities after carbonization.[23] Yet, further optimization is needed to minimize possible defects in the fibers.

In brittle materials, such as CFs, fracture instead of plastic deformation occurs under high tensile stress.[35] The "weakest link" theory states that fracture occurs at the weakest point in a CF.[36] Defects in a CF are classified into macroscopic defects such as pores or microscopic defects in the carbon structure.[37] The Weibull statistics can describe the distribution of the defects by the Weibull strength. **Table 4** provides an overview of the Weibull strengths (σ_0) and the Weibull modulus (m) of the fabricated CFs, the corresponding plots are shown in Figure S7, Supporting Information. The larger the value, the more uniformly the defects are distributed in the CF, that is, the better the homogeneity of the fiber is. The values found here were between $3.4 < m < 5.1$ with CF1000 prepared at a maximum temperature of 1000 °C showing the lowest Weibull modulus at $m = 3.4$, indicating lower homogeneity. Nevertheless, all m-values were in the range of commercial CFs from 4 to 10.[3,34,38]

Table 4. Summary of the determined Weibull strengths (σ_0) and the Weibull modulus (m) of the investigated CFs prepared at different maximum temperatures of carbonization. Weibull plots are shown in Figure S7, Supporting Information.

Sample ID	carbonization temperature [°C]	DR	σ_0 [GPa]	m [a.u.]	R^2
CF1000	1000	1.00	0.74	3.4	0.9551
CF1200	1200	1.00	1.04	5.1	0.9486
CF1400	1400	1.00	1.06	4.2	0.9293
CF1600	1600	1.00	0.91	5.0	0.9613

In line with the highest values for tensile strength and Yong's modulus, CF1400.3 (DR 1.05) showed the highest m-value of 5.1, which indicates that these fibers had a higher homogeneity compared to CF1400 (DR 1.00) with $m = 4.2$ and CF1400.2 (DR 1.01) with $m = 4.3$ (**Table 5**). Weibull statistics revealed that the process is stable and allows for the preparation of CFs with reproducible mechanical properties.

2.4. Carbon Fiber Morphology

Figure 2 shows the morphologies of the CFs carbonized at 1400 °C at different DRs during carbonization. All CFs showed a

Table 5. Summary of the values for σ_0 and m of CFs carbonized at 1400 °C with different draw ratio. The Weibull plots are shown in Figure S7, Supporting Information.

Sample ID	carbonization temperature [°C]	DR	σ_0 [GPa]	m [a.u.]	R^2
CF1400	1400	1.00	1.06	4.2	0.9293
CF1400.2	1400	1.01	1.30	4.3	0.9856
CF1400.3	1400	1.05	1.42	5.1	0.9040

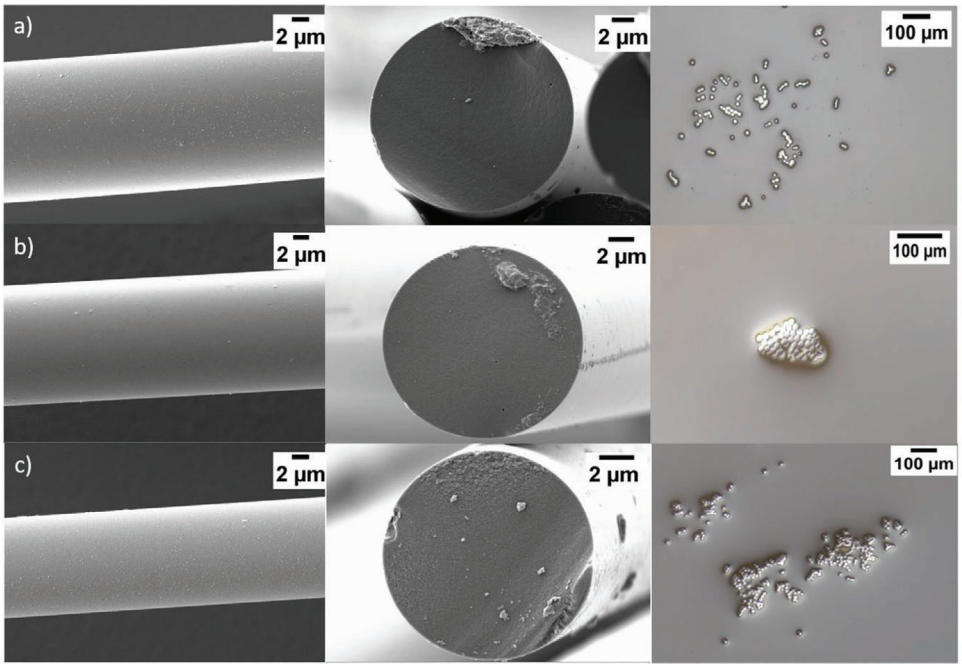

Figure 2. SEM micrographs of the surface and cross-section of CFs carbonized at 1400 °C with different draw ratio a) CF1400 (draw ratio = 1.00), b) CF1400.2 (draw ratio = 1.01), and c) CF1400.3 (draw ratio = 1.05).

uniformly round fiber cross-section without pores or voids. The surfaces of the fibers were smooth, fully compact, and without any visible defects and adhesions. The diameters of CFs were between 10–14 µm. The fibers showed slight fiber fusing after carbonization, originating from the spinning trials. In single filament measurement, the rarely occurring fiber fusing did not show any effect because the fibers were separated during sample preparation. The SEM images of fibers prepared at maximum carbonization temperatures between 1000 and 1600 °C revealed no differences in morphology (Figure S8, Supporting Information).

2.5. Carbon Fiber Structure

Elucidation of the structure of the CFs was performed by wide-angle X-ray scattering (WAXS) measurements. Values for the crystallite size (L_a, L_c) and interlayer spacing d_{002} were calculated by curve fitting of the (002) and (100) reflections. **Table 6** shows the calculated WAXS values of the CFs at the different maximum carbonization temperatures between 1000 and 1600 °C. With increasing carbonization temperature, the L_a-value increased from 3.00 to 3.87 nm while the L_c-value showed no significant increase; values ranged between 0.85 and 0.79 nm. Also, d_{002}, indicative of the degree of graphitization, remained between 0.375 and 0.363 nm. In comparison to PAN-based CFs, the interlayer spacing d_{002} decreased with increasing carbonization temperature.[18] **Table 7** summarizes the WAXS values of CFs resulting from continuous carbonization at 1400 °C with different DRs.

Table 6. Structural properties of CFs resulting from continuous carbonization from 1000 °C to 1600 °C. X-ray diffraction patterns are shown in Figure S9, Supporting Information.

Sample ID	carbonization temperature [°C]	DR	L_a [nm]	L_c [nm]	N_c	d_{002} [nm]
CF1000	1000	1.00	3.00	0.85	3.6	0.369
CF1200	1200	1.00	3.43	0.80	3.7	0.372
CF1400	1400	1.00	3.49	0.79	3.7	0.375
CF1600	1600	1.00	3.87	0.84	3.6	0.365

With increasing DR, the degree of preferred orientation of the crystallites along the fiber axis (P.O.) increased to 61%. The P.O. correlates with an increase in the Young's modulus from 74 ± 21 to 101 ± 18 GPa. No preferred orientation could be determined for the CF1400 fiber (DR = 1). By contrast, values for the crystallite size (L_a, L_c) and interlayer spacing d_{002} of CF1400.3 prepared by applying a DR of 1.05 differed significantly from those of the CF1400 fiber in that higher values for L_a, L_c and P.O., and a lower d_{002} value were observed. Generally, all d_{002} values were comparable to those of lignin-based CFs dry-spun from acetic acid (0.386 and 0.365 nm).[31] Overall, lignin-based CFs had a substantially lower tensile strength, Young's modulus, and P.O. than the PAN-based Toray T300CF (Table 3), which is also reflected by lower L_c and P.O., and higher L_a and d_{002} values.[34]

As displayed in Figure S11, Supporting Information, the Raman spectra of the CFs displayed the typical D-and G-bands. The intensity ratio (I_D/I_G) of the defect band (D1 band, 1340 cm^{-1}) and the graphite band (G band, 1590 cm^{-1}) depends on the carbonization temperature and provides information about defects in the graphite structure.[34,39–41] The lower the I_D/I_G ratio is, the lower the number of defects in the carbon structure is. With increasing maximum carbonization temperature, the I_D/I_G ratio decreased from 9.5 to 2.3 (−76%, **Table 8**), which is comparable to the literature known I_D/I_G ratio of lignin-based CFs (I_D/I_G = 2

Table 7. Structural properties of CFs resulting from continuous carbonization at 1400 °C with different DR. X-ray diffraction patterns are shown in Figure S10, Supporting Information.

Sample ID	carbonization temperature [°C]	DR	L_a [nm]	L_c [nm]	d_{002} [nm]	N_c	P.O. [%]
CF1400	1400	1.00	3.49	0.79	0.375	3.7	—
CF1400.2	1400	1.01	3.49	0.79	0.374	3.7	53
CF1400.3	1400	1.05	3.83	0.82	0.371	3.7	61
T300 (PAN-derived)	—	—	2.63	1.29	0.359	3.6	81

to 5).[31,42,43] All CFs showed a sharpening of the D-band with increasing temperature (Table S1, Supporting Information), which indicates the conversion of amorphous carbon regions to a more crystalline carbon phase. Clearly, an increase of the carbonization temperature led to better carbon-layer formation in the resulting CFs.

3. Conclusion

Continuous CFs were successfully produced from aqueous solutions containing 60 wt% ammonium lignosulfonate and 40 wt% PVP. Precursor multifilament fibers with 250 filaments were produced in a dry-spinning process and wound at 85 m min^{-1}. The precursor fibers were stabilized discontinuously in a drying oven at 250 °C applying a heating rate of 1 °C min^{-1}. The stabilized fibers were continuously processed into CFs on a pilot line. Increasing the DR in the carbonization process leads in an increase in tensile strength and Young's modulus. Continuous carbonization at 1400 °C with a draw ratio of 5% allowed for tensile strengths of 1.30 ± 0.32 GPa, a Young's modulus of 101 ± 18 GPa, and an elongation at break of 1.31 ± 0.23%. SEM images of the CFs showed a compact microstructure and a uniformly round fiber cross-section without pores or voids. Additional investigations of the stabilization and carbonization trials need to be carried out to further improve the mechanical properties of the lignin-based CFs.

4. Experimental Section

Materials: Ammonium lignosulfonate (ash content 5 wt%) was obtained from Borregaard (Norway). The additive polymer used was PVP K30 (Kollidon 30) with a weight-average molecular weight of 50.000 g mol^{-1} and a glass transition temperature of 171 °C, obtained from BASF SE (Germany).

Preparation of the Precursor Fibers: The dry spinning solution, consisting of 60 wt% ammonium lignosulfonates and 40 wt% PVP K30, was prepared by dissolving 350 g ammonium lignosulfonate and 150 g PVP in 1.4 L of water under stirring using a RW 20 digital stirrer by IKA-Werke GmbH and Co. KG (Germany). The rheology of the spinning solution was adjusted by heating to 40 °C by applying vacuum with a rotary evaporator. The complex viscosity, determined according to DIN 53019-4, was between 200–500 Pa s at a deformation of 10%, depending on the processing temperature. The spinning mass was filtered through a 20 µm mesh filter to remove residual particles. Dry-spinning (**Figure 3**(i)) was accomplished on a 1 kg scale on a pilot-scale line using a 250 capillaries spinneret (100 µm capillary diameter) through a 9 m spinning shaft (Figure S3, Supporting Information). The dosing was carried out with a gear pump (1.2 cm^3) with a rotational speed of 11 rpm and the spinning temperature was 22 °C. Before entering the spinneret, the spinning dope was passed through a 36 µm mesh filter. The exit speed at the spinneret was calculated to be 6.7 m min^{-1}, while the take-up speed on a laboratory winder manufactured by Georg Sahm GmbH and Co. KG (Germany) was 85 m min^{-1}. Figure S1, Supporting Information, gives an illustration of the dry spinning pilot line.

Stabilization: Oxidative thermostabilization (Figure 3(ii)) of the precursor fibers was realized discontinuously by heating in air up to 250 °C applying a heating rate of 1 °C min^{-1} in the drying oven. For this purpose, the fibers were deposited from the bobbin onto a foil and wound back onto a bobbin after stabilization (Figure S4, Supporting Information).

Carbonization: Continuous carbonization (Figure 3(iii)) of the stabilized fibers was carried out under nitrogen on a pilot carbonization line (Carbolite-Gero GmbH/Neuhausen) consisting of a low-temperature (LT)

Table 8. I_D/I_G values of CFs resulting from continuous carbonization at different maximum carbonization temperature.

Sample-ID	carbonization temperature [°C]	I_D/I_G
CF1000	1000	9.5
CF1200	1200	4.0
CF1400	1400	3.3
CF1600	1600	2.3

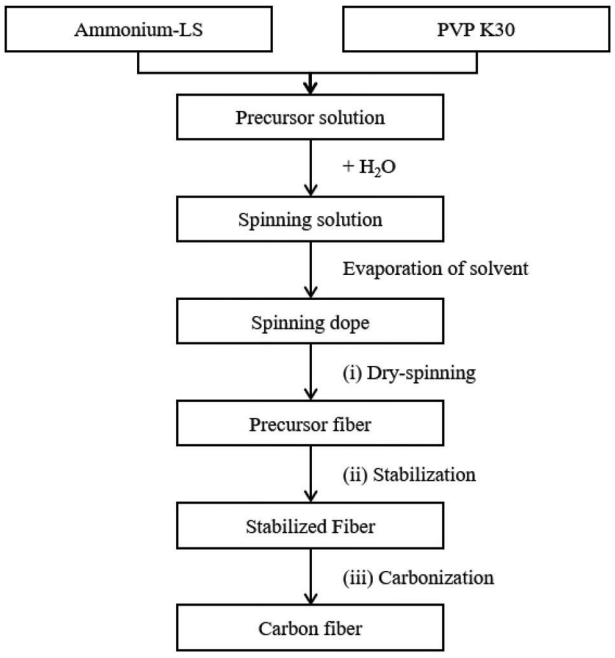

Figure 3. Preparation and processing of lignin-based CFs. LS = lignosulfonate, PVP = poly(vinylpyrrolidone).

and a high-temperature (HT) furnace (Figure S2, Supporting Information). The fiber samples were pyrolyzed at temperatures ranging from 300 to 750 °C in the LT furnace. The final temperature in the HT furnace was varied between 1000 and 1600 °C. All trials were carried out at a process speed of 0.4 m min^{-1}. Subsequently, the mechanical properties and the density of the fibers were determined.

Characterization: SEM was performed on a Hitachi SU70 microscope at an accelerating voltage of 20 kV and a working distance of 14 mm. All samples were sputter-coated with Pt/Pd prior. The fibers were placed in a sample holder (2 cm diameter) to study the sample surface. For studying the fiber cross-section, the samples were fractured. The rheology of the spinning dope was measured on an Anton Paar MCR 301 rheometer with a parallel-plate geometry. The plates diameter was 25 mm and the measuring distance was 0.5 mm. Measurements were carried out at temperatures between 45 and 15 °C with a deformation of 10% and shear rates of 100 to 1 rad s^{-1}. In addition to the complex viscosity ($|\eta^*|$), both the loss modulus (G'') and storage modulus (G') were determined. The rheological data at selected temperatures were superposed (time–temperature superposition) into a master curve at a temperature of 22 °C. The zero shear viscosity η_0 was calculated using the Carreau–Gahleitner model.[44] The mechanical properties of the CFs were measured according to EN ISO 5079 on a Favimat from Textechno (Mönchengladbach, Germany) at 20 °C. The mean value was obtained from at least 30 single filament measurements (measuring length: 12 mm, 0.5 mm min^{-1} test speed). Due to the brittleness of the fibers, the measuring length was reduced to 12 mm. The Young's modulus was determined in an elongation range of 0.2–0.4%. Densities of the fibers were determined at 22 °C in *n*-heptane/1,3-dibromopropane/tetrachloromethane gradient columns (three measurements). For WAXS, a Rigaku D/Max Rapid II operated at 40 kV and 30 mA with CuKα radiation ($\lambda = 0.154059$ nm) was used. A shine monochromator and an image plate detector were employed. The scanning rate was 0.2° min^{-1} with 0.1° scanning steps. Samples were placed in a fiber holder and measured for 5 h. All patterns were background corrected. The reflexes were fitted using between four and seven Pearson VII functions using the fitting software PDXL2 (Rigaku Co. Ltd.) to obtain the reflex position, and d_{002}-spacing for each sample. The crystallite sizes L_a und L_c were calculated using the Scherrer equation.[45] In this formula, K describes the Scherrer factor and θ_b is the Bragg-angle.

$$L = \frac{K \times \lambda}{B \times \cos\theta_b} \tag{1}$$

The degree of preferred orientation of the crystallites along the fiber axis (P.O.) for CFs was calculated using the width at half height of the reflection (B) according to the following formula.

$$\text{P.O.} = \frac{180° - B}{180°} \tag{2}$$

For Raman spectroscopy, a WITec alpha300 Raman microscope with ultra-fast imaging configuration, working at $\lambda = 532$ nm, was used. The Raman microscope was equipped with a UHTS300 spectrometer VIS, a YAG laser ($\lambda = 532$ nm; 50 mW), and an EMCCD camera. Curve deconvolution was achieved by Lorentzian curves using the Origin software for the determination of width at half height, the intensity ratio, and area ratio of the Raman bands.[39]

Supporting Information

Supporting Information is available from the Wiley Online Library or from the author.

Acknowledgements

Special thank goes to Ulrich Hageroth and Sabine Henzler for SEM and Raman measurements and Dr. Marc P. Vocht for the Raman analysis. The Author thank Dr. Hagen Altmann and Dr. Mark Steinmann for support. Financial support provided by Technikum Laubholz GmbH is gratefully acknowledged.

Open access funding enabled and organized by Projekt DEAL.

Conflict of Interest

The authors declare no conflict of interest.

Data Availability Statement

The data that support the findings of this study are available from the corresponding author upon reasonable request.

Keywords

carbon fibers, dry-spinning, lignosulfonates, tensile strength

Received: August 23, 2023
Revised: September 22, 2023
Published online: October 17, 2023

[1] The Global CF and CCMarket 2018 – Marketdevelopments, Trends, Outlook and Challenges (CCeV), https://composites-united.com/media/3988/eng_ccev_market-report_2019_short-version.pdf (accessed: September 2023)
[2] H. Mainka, O. Täger, E. Körner, L. Hilfert, S. Busse, F. T. Edelmann, A. S. Herrmann, *J. Mater. Res. Technol.* **2015**, *4*, 283.
[3] S. König, V. Bauch, C. Herbert, A. Wego, M. Steinmann, E. Frank, M. R. Buchmeiser, *Macromol. Mater. Eng.* **2021**, *306*, 2100484.
[4] M. M. Iovleva, V. N. Smirnova, G. A. Budnitskii, *Fibre Chem.* **2001**, *33*, 262.
[5] N.-D. Le, R. J. Varley, M. Hummel, M. Trogen, N. Byrne, *Mater. Today Sustainability* **2022**, *20*, 100251.
[6] H. Mao, X. Chen, R. Huang, M. Chen, R. Yang, P. Lan, M. Zhou, F. Zhang, Y. Yang, X. Zhou, *Sci. Rep.* **2018**, *8*, 9501.
[7] W. Fang, S. Yang, X.-L. Wang, T.-Q. Yuan, R.-C. Sun, *Green Chem.* **2017**, *19*, 1794.
[8] S.-C. Sun, Y. Xu, J.-L. Wen, T.-Q. Yuan, R.-C. Sun, *Green Chem.* **2022**, *24*, 5709.
[9] M. N. Collins, M. Nechifor, F. Tanasa, M. Zanoaga, A. Mcloughlin, M. A. Stróżyk, M. Culebras, C.-A. Teaca, *Int. J. Biol. Macromol.* **2019**, *131*, 828.
[10] S. Laurichesse, L. Avérous, *Prog. Polym. Sci.* **2014**, *39*, 1266.
[11] M. P. F. Graça, A. Rudnitskaya, F. Faria, D. Evtuguin, M. T. Gomes, J. Oliveira, L. Costa, *Electrochim. Acta* **2012**, *76*, 69.
[12] L. Rozite, J. Varna, R. Joffe, A. Pupurs, *J. Thermoplast Compos. Mater.* **2013**, *26*, 476.
[13] Y. Uraki, S. Kubo, N. Nigo, Y. Sano, T. Sasaya, *Holzforschung* **1995**, *49*, 343.
[14] J. F. Kadla, S. Kubo, R. A. Venditti, R. D. Gilbert, A. L. Compere, W. Griffith, *Carbon* **2002**, *40*, 2913.
[15] D. A. Baker, N. C. Gallego, F. S. Baker, *J. Appl. Polym. Sci.* **2012**, *124*, 227.
[16] Y. Jin, J. Lin, Y. Cheng, C. Lu, *Materials* **2021**, *14*, 3378.
[17] B. Saake, R. Lehnen, in *Ullmann's Encyclopedia of Industrial Chemistry*, Wiley, New York, **2007**, *21*, 21.
[18] E. Frank, L. M. Steudle, D. Ingildeev, J. M. Spörl, M. R. Buchmeiser, *Angew. Chem., Int. Ed.* **2014**, *53*, 5262.
[19] S. Kubo, J. F. Kadla, *J. Polym. Environ.* **2005**, *13*, 97.
[20] M. Thunga, K. Chen, D. Grewell, M. R. Kessler, *Carbon* **2014**, *68*, 159.

[21] P. Alexy, B. Kosi?Ková, G. Podstránska, *Polymer* **2000**, *41*, 4901.
[22] M. Zhang, *Carbon Fibers Derived from Dry-Spinning of Modified Lignin Precursors*, Clemson University, Clemson, SC **2016**.
[23] M. Zhang, A. A. Ogale, *Carbon* **2014**, *69*, 626.
[24] S. Otani, Y. Fukuoka, B. Igarashi, K. Sasaki (Nippon Kayaku Co Ltd), *US3461082A*, **1969**.
[25] S. P. Maradur, C. H. Kim, S. Y. Kim, B.-H. Kim, W. C. Kim, K. S. Yang, *Synth. Met.* **2012**, *162*, 453.
[26] K. Xia, Q. Ouyang, Y. Chen, X. Wang, X. Qian, L. Wang, *ACS Sustainable Chem. Eng.* **2016**, *4*, 159.
[27] A. Bengtsson, P. Hecht, J. Sommertune, M. Ek, M. Sedin, E. Sjöholm, *ACS Sustainable Chem. Eng.* **2020**, *8*, 6826.
[28] T. Nypelö, S. Asaadi, G. Kneidinger, H. Sixta, J. Konnerth, *Cellulose* **2018**, *25*, 5297.
[29] M. Mansmann, G. Winter, G. Pampus, N. Schon (Bayer AG), *US3723609*, **1973**.
[30] M. Mansmann (Bayer AG), *DE2118488A*, **1972**.
[31] J. Jin, J. Ding, A. Klett, M. C. Thies, A. A. Ogale, *ACS Sustainable Chem. Eng.* **2018**, *6*, 14135.
[32] T. Matsumoto, *Pure Appl. Chem.* **1985**, *57*, 1553.
[33] N. V. Salim, S. Blight, C. Creighton, S. Nunna, S. Atkiss, J. M. Razal, *Ind. Eng. Chem. Res.* **2018**, *57*, 4268.
[34] M. P. Vocht, A. Ota, E. Frank, F. Hermanutz, M. R. Buchmeiser, *Ind. Eng. Chem. Res.* **2022**, *61*, 5191.
[35] S. Zwaag, *J. Test Eval.* **1989**, *17*, 292.
[36] W. Weibull, *Ingenioersvetenskapsakad., Handl.* **1939**, *151*, 151.
[37] F. W. Zok, *J. Am. Ceram. Soc.* **2017**, *100*, 1265.
[38] K. Naito, Y. Tanaka, J.-M. Yang, Y. Kagawa, *Carbon* **2008**, *46*, 189.
[39] A. Sadezky, H. Muckenhuber, H. Grothe, R. Niessner, U. Pöschl, *Carbon* **2005**, *43*, 1731.
[40] A. C. Ferrari, J. C. Meyer, V. Scardaci, C. Casiraghi, M. Lazzeri, F. Mauri, S. Piscanec, D. Jiang, K. S. Novoselov, S. Roth, A. K. Geim, *Phys. Rev. Lett.* **2006**, *97*, 187401.
[41] S. Bernard, O. Beyssac, K. Benzerara, N. Findling, G. Tzvetkov, G. E. Brown, *Carbon* **2010**, *48*, 2506.
[42] M. Schreiber, S. Vivekanandhan, A. K. Mohanty, M. Misra, *ACS Sustainable Chem. Eng.* **2015**, *3*, 33.
[43] S. Wang, Z. Zhou, H. Xiang, W. Chen, E. Yin, T. Chang, M. Zhu, *Compos. Sci. Technol.* **2016**, *128*, 116.
[44] L. Reinders, S. Pfeifer, S. Kröner, H. Stolpmann, A. Renfftlen, L. C. Greiler, B. Clauß, M. R. Buchmeiser, *J. Eur. Ceram. Soc.* **2021**, *41*, 3570.
[45] P. Scherrer, in *Kolloidchemie Ein Lehrbuch* (Ed: R. Zsigmondy), Springer, Berlin **1912**, pp. 387–409.

